Chinese Journal of Polymer Science Vol. 35, No. 3, (2017), 407–421

Chinese Journal of Polymer Science

Plasticized Polymer Electrolyte Membranes Based on PEO/PVdF-HFP for Use as an Effective Electrolyte in Lithium-ion Batteries*

Pradeepa Prabakaran, Ramesh Prabhu Manimuthu**,
Sowmya Gurusamy and Edwinraj Sebasthiyan
School of Physics, Alagappa University, Karaikudi-630 004, Tamil Nadu, India

Abstract Plasticized polymer electrolytes were prepared using poly(ethylene oxide) (PEO)/poly(vinylidene fluoride-hexafluoro propylene) (PVdF-HFP) with lithium perchlorate ($LiClO_4$) and different plasticizers. XRD and FTIR spectroscopic techniques were used to characterize the structure and the complexation of plasticizer with the host polymer matrix. The role of interaction between polymer hosts and plasticizer on conductivity is discussed using the results of alternating current (a.c.) impedance studies. TG-DTA and SEM were used for thermal and physical characterizations. Maximum ionic conductivity (3.26×10^{-4} $S \cdot cm^{-1}$) has been observed for ethylene carbonate (EC)-based polymer electrolytes. Electrochemical performance of the plasticized polymer electrolyte is evaluated in $LiFePO_4$/plasticized polymer electrolytes (PPEs)/Li coin cell. Good performance with low capacity fading on charge discharge cycling is demonstrated.

Keywords X-ray diffraction; Impedance spectroscopy; Atomic force microscopy; Ionic conductivity; Dielectrics

INTRODUCTION

The world energy consumption, along with CO_2 emission, has been increasing exponentially during the past 50 years. The inevitably increasing fuel shortage, along with the public awareness of 'greenhouse' effects, has made it highly desirable to develop electric vehicles (EVs), hybrid electric vehicles (HEVs) and/or plug-in hybrid electric vehicles (PHEVs), instead of fossil fuel vehicles, with a low green house gas (GHG) emission. However, commercial applications of EVs will not be realized if advanced energy storage systems with an efficient energy saving and emission reduction cannot be successfully developed[1]. With no moving parts or noise and virtually without any pollution, batteries can convert chemical energy directly into electricity. They require little upkeep for potential large-scale applications. Among the several battery types, the lithium batteries (LIBs) have received intensive research and development focus because of their high energy density, long cycle life and superior environmental friendliness[2]. The research community is currently engaging in profuse efforts to achieve effective energy storage strategies which are the key for the exploitation of alternative energy and thus for the replacement of fossil fuels and traditional energy sources[3]. Lithium-ion battery dominates the market with its use in different electronic products, and even in hybrid electric vehicles in recent years[4–6].

To achieve an efficient battery system, good performance of battery components is necessary. Therefore, development of superior components is paramount for next generation batteries. Among the battery components, one important component is the electrolyte. Polymer electrolytes on their own, though shapeable, versatile, flexible, tough, light weight and processable, have low room temperature (RT) ionic conductivity (σ) in the

* This work was financially supported by the UGC-BSR, New Delhi, India.
** Corresponding author: Ramesh Prabhu Manimuthu, E-mail: mkram83@gmail.com
Received July 5, 2016; Revised October 14, 2016; Accepted October 18, 2016
doi: 10.1007/s10118-017-1906-9

range of 10^{-6} S·cm^{-1} to 10^{-8} S·cm^{-1} due to low effective carrier mobility. Several strategies aimed at improving RT conductivity while preserving the inherent advantages of polymers have been explored in the last two decades. Solid polymer electrolytes (SPEs) promise the potential to replace organic liquid electrolytes and thereby improve the safety of next-generation high-energy batteries[7, 8]. However, their low ionic conductivities have restricted the mass use of this type of electrolytes in batteries[9]. Some approaches such as addition of micron/nano-sized filler particles, use of co-polymers and blends, synthesis of cross linked and branched structure, use of organic solvents in polymer matrices (gel or plasticized electrolytes), *etc*. have been tested and succeeded to enhance the ionic conductivity[10–14]. Among these approaches, gel or plasticized polymer electrolytes (GPEs/PPEs) are regarded as prospective alternative for traditional liquid electrolytes used in batteries, since gels possess both cohesive properties of solids and the diffusive properties of liquids. The electrolyte leakage from a battery can be to a large extent prevented with this gel or plasticized electrolytes as the liquid component is trapped in the polymer matrix and therefore the membrane virtually looks like a solid in character. This unique characteristic makes the gel find various important applications including polymer electrolytes[15, 16].

Low evaporating solvents such as ethylene carbonate (EC), propylene carbonate (PC), dimethyl formamide (DMF), diethyl phthalate (DEP), diethyl carbonate (DEC), methyl ethyl carbonate (MEC), dimethyl carbonate (DMC) and alkyl phthalates have been commonly investigated as plasticizers solvents for the gel electrolytes[17]. These plasticizers will increase the flexibility of the polymer chain and enhance the ionic conductivity. Plasticization has been recognized as one of the effective and efficient routes available for reducing the crystallinity and also enhancement of the amorphous nature of the solid polymer electrolytes. The effect of plasticizer on the polymer electrolyte strongly relies on the specific nature of the plasticizer, including the dielectric constant, polymer-plasticizer interaction and ion plasticizer coordination[18]. It was generally observed that up to 80% of solvent could be trapped into the polymer matrix. The high permittivity solvents allowed a greater dissociation of the lithium salt and increased the mobility of the cation[17].

Mostly, poly(ethylene oxide) (PEO) matrix based complexes have been widely used in this direction. The PEO has low lattice energy, low glass transition temperature, high solvating power for alkali metal salts and an ease to form flexible type film. These facts make it an impending polymer in preparation of the SPEs. Among the ionic conducting polymers, PVdF-HFP copolymer was found to meet all the requirements for use as the polymer host in GPE in terms of electrochemical stability and performance, processability, and safety. PVdF-HFP contains amorphous domains (HFP) capable of trapping large amounts of liquid electrolytes, and crystalline regions (VdF) which provide chemical stability and sufficient mechanical integrity for the processing[19]. The salt lithium perchlorate ($LiClO_4$) was chosen because of its lowest dissociation energy[20] and its low lattice energy of 723 kJ·mol^{-1}, among the various inorganic salts, which in turn lead to high ionic conductivity. The objective of this work is to understand how organic additives influence the structural, electrochemical, thermal and morphological properties. Table 1 provides comparative information on the differences in the functionality of each plasticizer.

Table 1 Overview of the reported experimental results considering the conducting nature of plasticized polymer electrolytes

Polymer matrix	Plasticizer	Ionic conductivity (S·cm^{-1})	Reference
PEO	EC	1.6×10^{-4}	[21]
PEO	EC-PC	1.2×10^{-4}	[22]
PVdF-HFP	TG	4.9×10^{-4}	[23]
PEO/PVdF-HFP/$LiClO_4$	PC-EC	1.30×10^{-4}	[24]
PEO/PVdF-HFP/$LiClO_4$	PC	2.39×10^{-4}	[25]
PEO/PVdF-HFP/$LiClO_4$	EC	3.26×10^{-4}	Present work

Based on our previous work[25], PEO (6.25 wt%), PVdF-HFP (18.75 wt%), $LiClO_4$ (8 wt%), PC (67 wt%) were found to be an optimized composition as it achieved highest ionic conductivity of 2.39×10^{-4} S·cm^{-1} at room temperature. Although the conductivity is comparable with literature reports for solid polymer electrolytes

(SPEs), it is still insufficient for application in electrochemical devices. Hence, in this work, we have plasticized (65 wt%) of ethylene carbonate as plasticizer with PEO (6.25 wt%), PVdF-HFP (18.75 wt%) and $LiClO_4$ (8 wt%) to enhance conductivity value and use the membrane in coin cell fabrication. The main goal of the present work is to achieve a low capacity fading with chemically more stable polymers and to investigate the use of plasticized polymer electrolytes in lithium batteries. Results are presented, discussed and compared with reports found in the literature.

EXPERIMENTAL

Materials Used

Poly(ethylene oxide) with an average molecular weight MW ~ 8000 and poly(vinylidene fluoride-hexafluropropylene) with an average molecular weight MW ~ 1.1×10^5, were purchased from Sigma Aldrich Chemicals Limited, USA. Plasticizer such as propylene carbonate (PC), ethylene carbonate (EC), γ-butyrolactone (GBL), diethyl carbonate (DEC) and dimethyl carbonate (DMC) were purchased from E-Merck, Germany. These were used as starting materials for the polymer electrolyte preparation.

Preparation

The obtained PEO, PVdF-HFP and $LiClO_4$ were dried in vacuum oven at 55 °C for 4 h to remove the moisture. The composition of polymers was fixed as PEO (6.25 wt%), PVdF-HFP (18.75 wt%), $LiClO_4$ (8 wt%), and it was found to be an optimized composition as it achieved highest ionic conductivity reported in our previous work[25] when complexed with 67 wt% of as-received PC, EC, GBL, DEC and DMC. The gel based electrolytes were prepared by solution casting technique with acetone as a solvent. The above composition of lithium salt, plasticizer and the polymers PEO, PVdF-HFP were dissolved at room temperature respectively. After that, the polymer solution was stirred continuously for 24 h and slowly evaporated at 40 °C for obtaining a homogeneous solution. The film was cast by spreading the suspension on a well cleaned petri dish. The polymer films were dried at room temperature in a vacuum oven for 24 h in order to evaporate the residual solvents present in the polymer films. This procedure provides mechanically stable, free standing and flexible films. Chemical storage, film casting and cell assemblies were performed in the argon atmosphere.

Cell Assembly

Plasticized polymer electrolyte exhibiting a high ionic conductivity was tested in the $LiFePO_4$/PPE/Li half cell configuration. The cathode was prepared by mixing $LiFePO_4$ (active material), Super P Li carbon by Timcal (conductivity additive) and PVdF (binder) in the weight ratio 80:10:10 using *N*-methyl pyrrolidone (NMP) as a solvent. Then the homogenous viscous slurry was coated on the aluminum (Al) foil using doctor blade technique with the thickness of 25 μm. The resulting electrode was dried in a vacuum oven at 80 °C overnight to remove the solvent; as prepared dried electrode was pressed in between twin rollers to improve the adherence of the coating to the Al foil. Before cell assembly, the desired size of the active electrode (loading merely 8 mg) was dried in a vacuum oven at 80 °C for 12 h to remove the residual solvent traces present in the electrodes. The activation of the prepared electrolytes and the fabrication of coin type cells were carried out in an argon-filled glovebox with the oxygen and moisture level as < 0.1 ppm.

Characterization Techniques

The amorphousness of the polymer electrolytes has been investigated by XRD analysis with the help of X'pert PRO PANalytical X-ray diffractometer. The data were collected in the range of diffraction angle 2θ from 10° to 80° at the scanning rate of 0.05 (°)·s^{-1} at room temperature. The complex formation between the polymer and the salt has been confirmed by FTIR spectra using SPECTRA RXI, PerkinElmer spectrophotometer in the range of 400–4000 cm^{-1}. The prepared films were subjected to alternating current (a.c.) impedance analysis, in order to calculate the ionic conductivity with the help of stainless steel blocking electrodes using a computer controlled micro auto lab type III potentiostat/galvanostat in the frequency range of 100 Hz–300 kHz over the temperature range of 303–343 K. Thermal stability of the polymer electrolyte was carried out by thermogravimetric and differential thermal analysis (TG-DTA) by using PYRIS DIAMOND from room temperature to 500 °C at a

heating rate of 10 K·min^{-1} in nitrogen atmosphere. Mettler Toledo differential scanning calorimeter (DSC) (822e) instrument was employed to study the phase changes. The surface morphology of the electrolyte film was examined by Hitachi S3000H scanning electron microscope. Roughness parameter was measured using A100SGS atomic force microscope. The galvanostatic charge-discharge tests were conducted between 2.5 and 4.5 V at room temperature using BTS XWJ, Neware Tech. Co. battery testing equipment.

RESULTS AND DISCUSSION

X-ray Diffraction Studies

Figure 1 shows the respective diffraction patterns of pure PEO, PVdF-HFP, $LiClO_4$ and PC, EC, GBL, DEC and DMC based complexes. Two broad peaks are found at $2\theta = 19.20°$ and 23.15° corresponding to the reflections of (120) and (010) planes respectively, which confirms the semi crystalline nature of PEO. The peaks at 17.5°, 18.5°, 20.2° and 39° correspond to (100), (020), (110) and (021) respectively which reveal the semi crystalline nature of PVdF-HFP shown in Fig. 1(b), and Fig. 1(c) of $LiClO_4$ shows high intense peaks at angles $2\theta = 21.7°$, 23.74°, 26.56°, 32.16° and 36.25° corresponding to the lattice planes (101), (110), (200), (201) and (210) respectively [JCPDS:30-0751]. The crystallinity of these polymers was significantly reduced and the peaks were broadened. It indicates that the addition of plasticizer and lithium salts in the polymer can suppress the crystallinity of the polymer. Also, the characteristic peaks of PEO shift towards the lower angle side with significant broadening on addition of the plasticizer. This shift indicates an increase in interplaner spacing of the (100) plane[26]. Figures 1(d)–1(h) reveal that the amorphous nature is predominant in the complex.

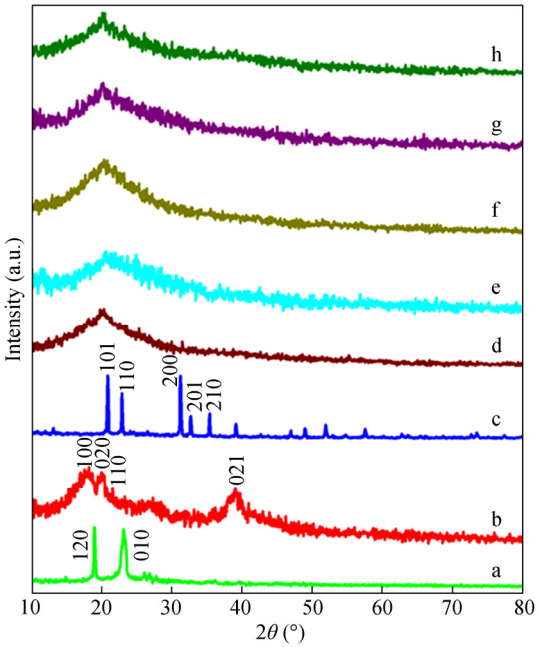

Fig. 1 XRD patterns of (a) pure PEO, (b) pure PVdF-HFP, (c) pure $LiClO_4$, (d) PEO (6.25)/PVdF-HFP (18.75)/$LiClO_4$ (8)/PC (67), (e) PEO (6.25)/PVdF-HFP (18.75)/$LiClO_4$ (8)/EC (67), (f) PEO (6.25)/PVdF-HFP (18.75)/$LiClO_4$ (8)/GBL (67), (g) PEO (6.25)/PVdF-HFP (18.75)/$LiClO_4$ (8)/DEC (67) and (h) PEO (6.25)/PVdF-HFP (18.75)/$LiClO_4$ (8)/DMC (67)

A fully amorphous morphology produces greater polymer flow and ionic diffusivity. High ionic conductivity can be obtained in amorphous polymers having highly flexible backbones and low glass transition temperature. It is due to the addition of plasticizers such as PC, EC, GBL, DEC and DMC. Upon adding different plasticizers, the polymers undergo significant structural reorganization. The degree of crystallinity of pure PEO, PVdF-HFP and $LiClO_4$ is found as 52.5%, 30% and 64.4%, respectively. It is also determined for PC,

EC, GBL, DEC and DMC based complexes as 35%, 33%, 40%, 48% and 53%, respectively. There was a decrease in the relative intensity of the apparent peaks with adding plasticizers. These results can be interpreted by considering the correlation between the height of the peak and the degree of crystallinity. This shows that the degree of crystallinity of the prepared samples decreases with different plasticizers, with the EC based electrolyte having reduced crystallinity. This is due to the existence of larger free volume and flexibility of total chain segmental motion in the polymer electrolyte[27]. Most of the peaks pertaining to $LiClO_4$ disappeared in the complexes, which indicates the complete dissolution of the salt in the polymer matrix. The above analysis concludes that the ion conduction takes place in the amorphous region, which was due to the incorporation of plasticizers, and it is confirmed that the complexation has occurred in the polymer hosts.

FTIR Spectroscopic Analysis

Figure 2 shows the FTIR spectra of the pure PEO, PVdF-HFP, plasticizer and their complexes respectively. The complexation between the blend polymer components can either shift or diminish intensity in the polymer peak frequencies. A large broad band at 2962 and 2823 cm^{-1} of PEO is shifted to (2959, 2969, 2972, 2981, 2986 cm^{-1}), (2832, 2845, 2829, 2821, 2826 cm^{-1}) in the complexes respectively. Two narrow bands of lower intensity at 2735 and 2695 cm^{-1} are inherent bands of asymmetric (C—H) stretching of CH_2 of PEO[28]. The bands at 2238, 2163 and 1967 cm^{-1} which are characteristic of PEO[29] get shifted to (2250, 2242, 2244, 2251, 2239 cm^{-1}), (2174, 2179, 2167, 2159, 2152 cm^{-1}) and (1972, 1969, 1976, 1980, 1984 cm^{-1}). The band at 1483 cm^{-1} is attributed to the C—H bending of CH_2 in PEO shifted at (1486, 1492, 1471, 1508, 1483 cm^{-1}) in the complexes.

A very small intensity band at 1799 cm^{-1} corresponds to the ether oxygen group of PEO[30]. The bands at around 1359 and 1343 cm^{-1} are assigned to CH_2 wagging and CH_2 bending, respectively, which are characteristic of PEO shifted in the complexes at (1363, 1369, 1361, 1351, 1355 cm^{-1}), (1346, 1342, 1351, 1358, 1350 cm^{-1}). The relatively small band at around 1236 cm^{-1} is assigned to CH_2 symmetric twisting of PEO and these peaks are found at (1237, 1233, 1235, 1235, 1230 cm^{-1}) in the complexes. The characteristic vibrational band at 1100 cm^{-1} was assigned to C—O—C (symmetric and asymmetric) stretching of PEO and are found at (1105, 1098, 1112, 1089 cm^{-1}). The two bands near 947 and 845 cm^{-1} are assigned to CH_2 rocking vibrations of methylene groups and are related to helical structure group of PEO. Apart from this, the mode responsible for the band at 845 cm^{-1} is primarily due to the CH_2 rocking motion with a little contribution from C—O stretching motion of PEO while the bands at 947 cm^{-1} originate primarily in the C—O stretching motion with some CH_2 rocking motion[31] and these bands are shifted to (845, 827, 852, 850, 841 cm^{-1}) and (952, 968, 944, 948, 946 cm^{-1}).

The vibrational peaks at 502 and 416 cm^{-1} are assigned to the bending and wagging vibrations of $-CF_2$ respectively and get shifted to (499, 511, 497, 492, 499 cm^{-1}) and (422, 512, 418, 424, 430 cm^{-1}). The crystalline phase of the PVdF-HFP polymer is identified by the vibrational bands at 985, 763 and 608 cm^{-1} which get shifted to (993, 982, 991, 996, 979 cm^{-1}), (771, 769, 767, 762, 773 cm^{-1}) and (617, 619, 622, 613, 611 cm^{-1}).

The peaks at 1173 and 1390 cm^{-1} are assigned to the symmetrical stretching of $-CF_2$ and $-CH_2$ groups respectively[32]. The peak at 881 cm^{-1} is assigned to the vinylidene group of the polymer and is shifted to (883, 876, 889, 881, 885 cm^{-1}). The band at 625 cm^{-1} corresponds to the ClO_4^- anion[33] which is present in the complexes. Fermi resonance occurred due to the coupling of two fundamental vibrational modes or the interaction between fundamental vibrations and overtones. The peaks at 1486, 1340 cm^{-1} of PC get shifted to 1484, 1348 cm^{-1} in Fig. 2(i). The C—O stretching vibration of PC that occurred at about 1300–1100 cm^{-1} completely disappeared. Broad peaks that occurred at 1645 and 879 cm^{-1} are assigned to $C=CF_2$ vibrations of vinylidene group. The absorption peaks at 2906 and 2978 cm^{-1} are assigned to asymmetric stretching vibrations of methyl group in PC[34]. The vibrational peaks at 1488, 1173, 1155, 774 cm^{-1} of EC get shifted to 1490, 1186, 1143, 782 cm^{-1} in Fig. 2(j). Sharp vibrational peaks at 1774 and 1789 cm^{-1} are assigned to C=O stretching vibrations of EC which have been shifted to 1770 cm^{-1} and they have been split into two small peaks, which are attributed to the Fermi resonance of the C=O stretching mode with an overtone of the ring breathing mode and

the existence of short-range ordering of the molecular orientation that originated from the dipole-dipole coupling of two EC molecules[35, 36]. The peaks at 2035, 1462, 676 cm^{-1} of GBL; 2049, 1649, 625 cm^{-1} of DEC; 1450, 1280, 1100, 920 cm^{-1} of DMC; are shifted to 2031, 1651, 632, 2031, 1462, 678, 1452, 1332, 1076 and 931 cm^{-1} in the spectra of the complexes, respectively. It is also observed that few vibrational peaks are shifted in both the lower and higher frequency regions, which may be due to the halogen substituent compounds or its high electronegative character. In such cases, significant shifting of the C—H frequencies occurs, and the direction of the shift is independent on the location of the C—H bond and whether the halogen increases (high frequency) or decreases (lower frequency) the electron density in the C—H bond[37]. The peaks at 2835, 1023, 1100, 570 cm^{-1} in the spectrum of PC-based complex, 1852, 1626, 1211, 889 cm^{-1} in the spectrum of EC-based complex; 521, 486 cm^{-1} in the spectrum of GBL-based complex; 2742, 1237, 821, 733 cm^{-1} in the spectrum of DEC-based complex and 1086, 620 cm^{-1} in the spectrum of DMC-based complex are absent. New peaks at 2634, 2332, 1878, 1513 and 2570 cm^{-1} are found to appear in the spectra of the complexes (D1) PEO (6.25)/PVdF-HFP (18.75)/$LiClO_4$ (8)/PC (67); (D2) PEO (6.25)/PVdF-HFP (18.75)/$LiClO_4$ (8)/EC (67); (D3) PEO (6.25)/PVdF-HFP (18.75)/$LiClO_4$ (8)/GBL (67); (D4) PEO (6.25)/PVdF-HFP (18.75)/$LiClO_4$ (8)/DEC (67) and (D5) PEO (6.25)/PVdF-HFP (18.75)/$LiClO_4$ (8)/DMC (67), respectively. Thus the above analysis confirmed the complex formation in the developed electrolytes.

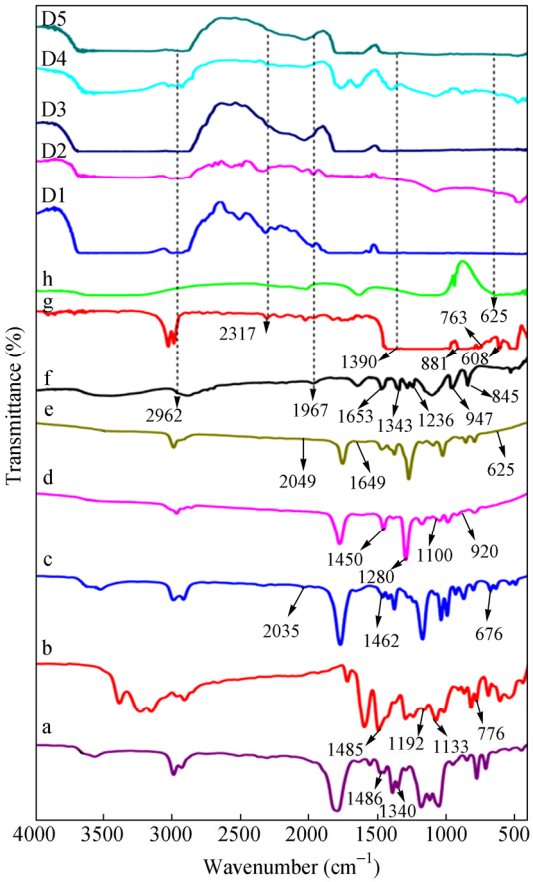

Fig. 2 FTIR spectra of (a) pure PC, (b) pure EC, (c) pure GBL, (d) pure DEC, (e) pure DMC, (f) pure PEO, (g) pure PVdF-HFP, (h) pure $LiClO_4$, (D1) PEO (6.25)/PVdF-HFP (18.75)/$LiClO_4$ (8)/PC (67), (D2) PEO (6.25)/PVdF-HFP (18.75)/$LiClO_4$ (8)/EC (67), (D3) PEO (6.25)/PVdF-HFP (18.75)/$LiClO_4$ (8)/GBL (67), (D4) PEO (6.25)/PVdF-HFP (18.75)/$LiClO_4$ (8)/DEC (67), (D5) PEO (6.25)/PVdF-HFP (18.75)/$LiClO_4$ (8)/DMC (67)

Ionic Conductivity

The ionic conductivities were calculated using the relation $\sigma = \ell/R_b A$, where ℓ is the thickness, R_b is bulk

resistance and A is the known area of the electrolyte film. The impedance responses are typical of the electrolytes where the bulk resistance (R_b) is the major contribution to the total resistance and only a minor contribution comes from grain boundary resistance. In the present work, the high frequency semicircle does not appear for all the plasticized systems studied. This phenomena also found in many plasticized systems in the literature[38, 39] are quite reasonable since the facile ion mobility in liquid and gel type electrolyte systems compared with solid polymer electrolytes, implies that the ion possesses small dielectric relaxation time and hence the inconsequential capacitative effect of the bulk electrolyte in the spectrum.

In Fig. 3 it is observed that impedance response of PPEs at a temperature between 30 and 70 °C (the minimum and maximum temperatures studied here) is in the form of a straight line inclined about 45° with respect to the real axis from high to lower frequencies.

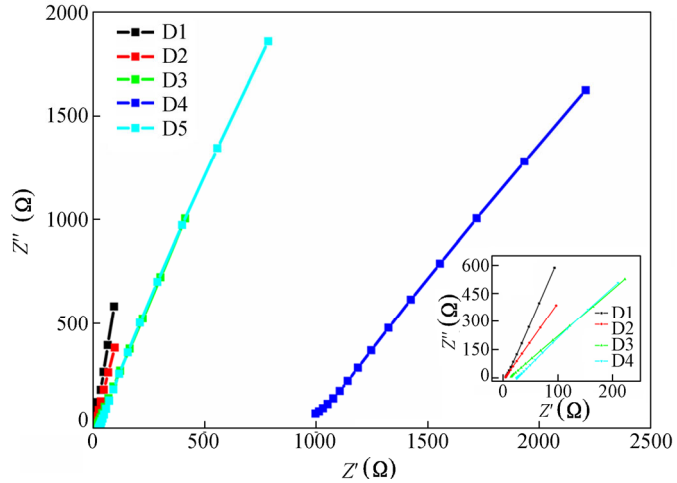

Fig. 3 Room temperature complex impedance plots of the prepared samples

This type of behavior is typical for a PPE sandwiched between two quasi-blocking electrodes. At 70 °C, it is observed that ionic resistance of PVdF-HFP/PEO decreases considerably with a shift of the inclined spike to higher frequency. It is observed (Fig. 6) that at temperatures above 60 °C, the crystalline segments of PEO melts, increasing the overall mobility of ions in the electrolyte. Compared to $LiClO_4$, the ionic resistance of PPE activated with plasticizers is seen to be very low even at the lower temperature of 25 °C. This implies that incorporation of plasticizer significantly reduces the electrolyte resistance due to its lower viscosity, and enhances the mobility of Li^+ ions in the electrolyte[40].

Plasticizer molecules being relatively small in size compared with polymer molecules penetrate the polymer matrix and establish attractive forces with the chain segments. These attractive forces reduce the cohesive forces between the polymer chains and increase the segmental mobility, which enhance the conductivity and the discharge time. The increase in conductivity value with the addition of same amount of different plasticizers (EC, PC, GBL, DEC, DMC) is in the following order: DEC < DMC < GBL < PC < EC with their dielectric constants 89.78 > 66 > 39 > 3.12 > 2.82. The conductivities of these electrolytes critically depend on the physical properties of the plasticizer such as its viscosity and dielectric constant[41]. Plasticizers with high dielectric constant dissociate more salt by increasing the relative permittivity of the system while plasticizers with high viscosities impede the mobility of ions. The plasticizers are also known to lower the T_g of the polymer host thereby increasing the polymer chain mobility and to lower the crystallinity of some polymers.

The maximum conductivity is obtained for the film containing EC, as EC is less viscous (1.90 mPa·s) and also the dielectric constant (ε = 89.78) is greater than that of the other plasticizers used. Also EC is a solid material at room temperature with a molecular weight of 88.05 g. The combined effects of the possession of viscosity as well as dielectric constant are responsible for the increase in conductivity. Thus EC based PEO/PVdF-HFP/$LiClO_4$ system offers maximum conductivity 3.26×10^{-4} S·cm^{-1} compared to other plasticizers

such as PC, GBL, DMC and DEC.

The Arrhenius type conductivity behavior was suggested since the ionic conductivity increased linearly with a slight non-linearity at high temperatures. The Arrhenius equation can be described as $\sigma = \sigma_0 \exp(-E_a/kT)$ where σ is the ionic conductivity, σ_0 the pre-exponential factor, E_a the activation energy and k the Boltzmann's constant. As the conductivity plot fits well with the Arrhenius equation (Fig. 4), the activation energies (E_a) of plasticized electrolyte membranes are calculated and listed in Table 2.

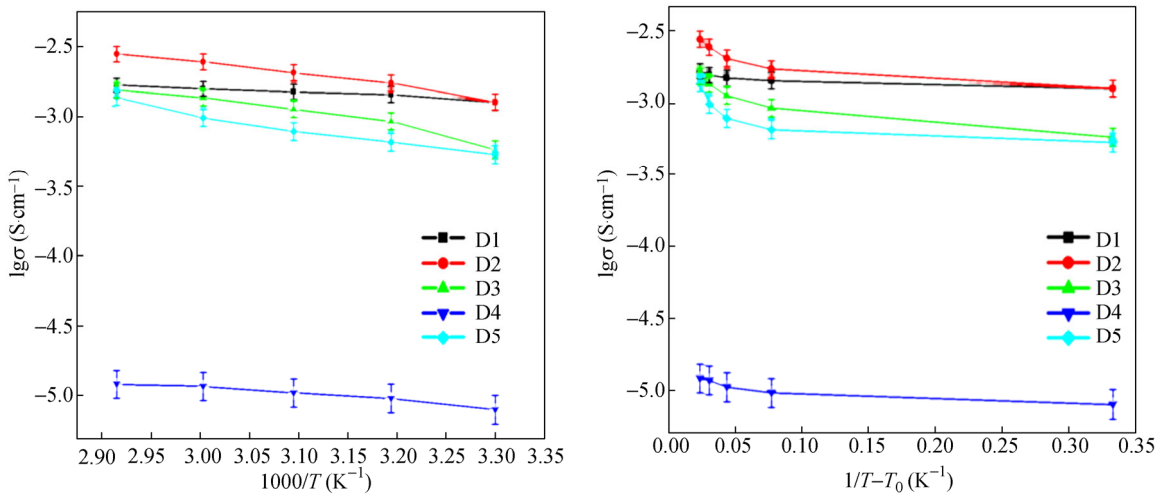

Fig. 4 Temperature dependent ionic conductivity of the prepared samples

Table 2 Ionic conductivity, activation energy and porosity values for PC, EC, GBL, DEC and DMC (67 wt%) complexed with PEO (6.25)/PVdF-HFP (18.75)/$LiClO_4$ (8) polymer electrolyte systems

Film	Plasticizers	Activation energy (E_a)	Porosity (%)	Ionic conductivity values at different temperatures (S·cm^{-1})				
				303 K	313 K	323 K	333 K	343 K
D1	PC	0.04	1.54	2.39×10^{-4}	2.56×10^{-4}	2.71×10^{-4}	2.84×10^{-4}	2.91×10^{-4}
D2	EC	0.18	5.02	3.26×10^{-4}	4.43×10^{-4}	5.49×10^{-3}	6.57×10^{-3}	7.67×10^{-3}
D3	GBL	0.34	1.25	7.91×10^{-5}	9.57×10^{-5}	7.81×10^{-4}	9.77×10^{-4}	1.54×10^{-3}
D4	DEC	0.02	0.75	5.33×10^{-5}	6.23×10^{-5}	1.04×10^{-4}	1.15×10^{-4}	1.19×10^{-4}
D5	DMC	0.18	1.08	5.76×10^{-5}	9.50×10^{-5}	1.12×10^{-4}	1.30×10^{-4}	1.37×10^{-4}

It was observed that the EC (67 wt%) sample possessed the lowest E_a value among the plasticized electrolyte membranes investigated. The low E_a values for all the hybrid electrolyte samples suggest that they are ionic charge carriers with fast diffusion. This observation revealed that the main transportation path in ionic movement was due to thermally activated ionic hopping instead of polymer segments[42]. Due to increase of temperature the viscosity of electrolyte decreases and finally the material changes into amorphous phase, which results in increase of free volume and favorable ion conducting paths in thermally activated dynamical medium.

When temperature is increased, the vibrational energy of a segment is sufficient to push against the hydrostatic pressure imposed by its neighboring atoms and create a small amount of space surrounding its own volume in which vibrational motion can occur. Therefore, the free volume around the polymer chain causes the mobility of ions and polymer segments and, hence, the conductivity. Hence, the increment of temperature causes the increases in conductivity due to the increased free volume and their respective ionic and segmental mobility. This increase in free volume would facilitate the motion of ionic charge. In the present case, there is a little possibility of ion transport through segmental movement of ions since the hybrid blend electrolytes follow the Arrhenius-type behavior (Fig. 4)[43]. Since the hybrid plasticized electrolytes can retain enough solvent for coordination with the Li^+ cations and the carbonyl solvents are more suitable for coordination with the Li^+ cations, most of the Li^+ ions movements take place through the liquid electrolyte filled in pore channels and through the swollen amorphous areas. Both factors significantly contributed to the ionic conductivity.

TG-DTA Analysis

Thermal degradation behavior of conducting polymers is very important for their potential applications. To investigate the thermal stability of the newly obtained polymer, Thermogravimetric (TG) analysis and differential thermogravimetric analysis (DTA) experiments were performed under a nitrogen stream[44]. Figure 5 shows the TG-DTA curves of EC, PC, GBL, DMC and DEC based PEO (6.25)/PVdF-HFP (18.75)/$LiClO_4$ (8) system. In the present study, the samples exhibit a gradual weight loss of about 11%–20% during an initial heating up to 110 °C, which was considered as the result of moisture from the electrolytes at the time of loading the samples.

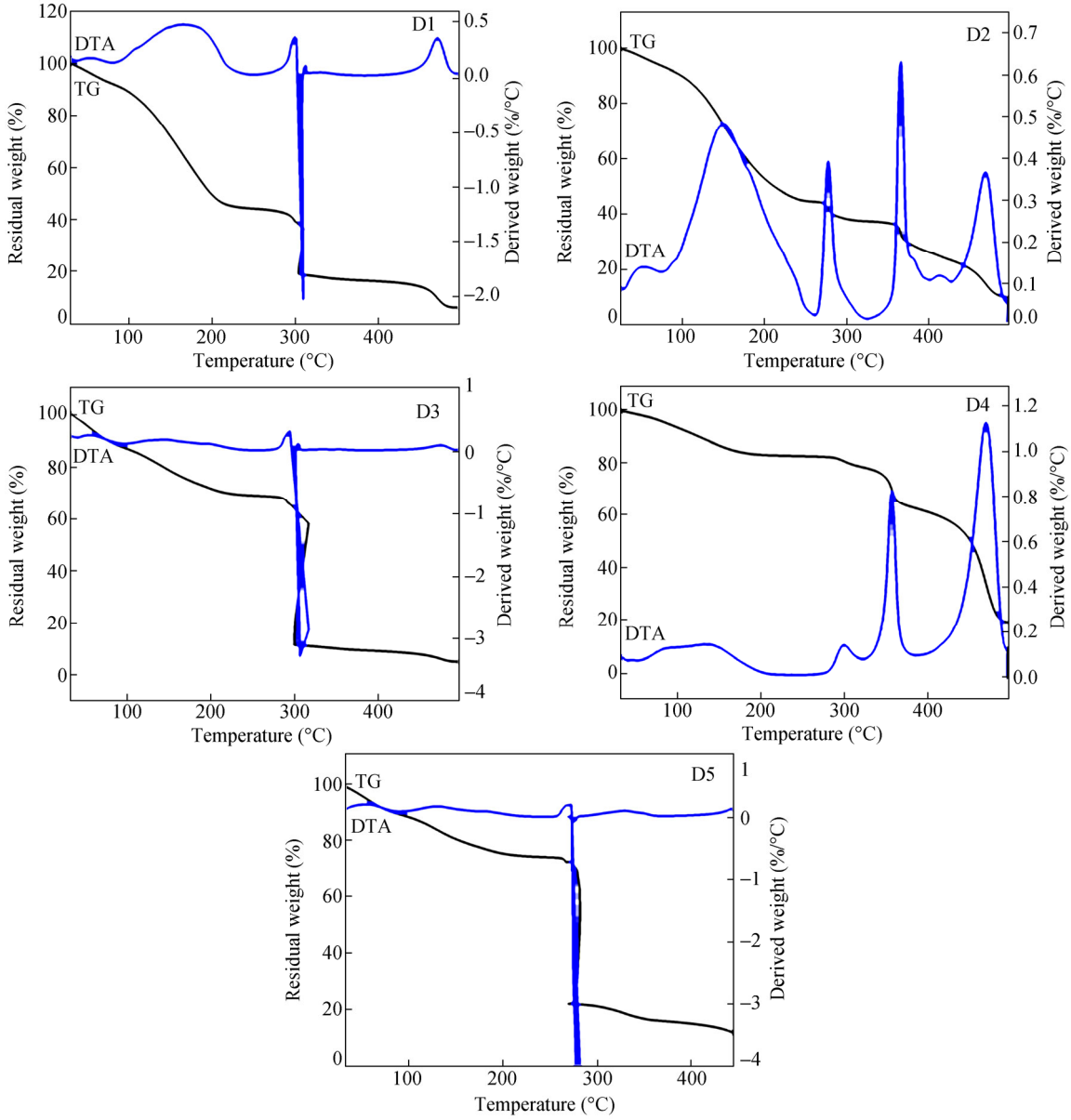

Fig. 5 TG-DTA analyses of the prepared complexes: (D1) PEO (6.25)/PVdF-HFP (18.75)/$LiClO_4$ (8)/PC (67), (D2) PEO (6.25)/PVdF-HFP (18.75)/$LiClO_4$ (8)/EC (67), (D3) PEO (6.25)/PVdF-HFP (18.75)/$LiClO_4$ (8)/GBL (67), (D4) PEO (6.25)/PVdF-HFP (18.75)/$LiClO_4$ (8)/DEC (67), (D5) PEO (6.25)/PVdF-HFP (18.75)/$LiClO_4$ (8)/DMC (67)

From the TG curves, it was observed that the first decomposition occurred at 213, 270, 210, 262 and 215 °C for EC, PC, GBL, DMC and DEC complexes respectively with the corresponding weight loss of 56% for EC-based complex, 54% for PC, 30% for GBL, 20% for DMC and 25% for DEC. After the first decomposition, there is a rapid weight loss of about 20%–56% in the temperature range of 220–270 °C for EC, PC, GBL, DEC complexes and 282 °C for DMC based complex. The complete decomposition of the sample takes place between 480 and 500 °C with the corresponding weight loss of about 75%–90%. This may be due to the decomposition of polymers and the evaporation of plasticizers.

It is observed from DTA curves that the decompositions of PEO/PVdF-HFP are also accompanied with the exothermic peaks in the range of 56–166 °C and large one in the range of 329–470 °C concurrent with the weight losses. This is attributed to the volatilization of monomers and oligomers adsorbed in the matrix, which may be responsible for the initial weight loss[45–47]. Hence, one can conclude that from the TG curves, the prepared electrolytes are decomposed above 270 °C except EC-based complex. This shows better stability of PEO/PVdF-HFP/EC plasticized electrolyte system. The decomposition temperature for EC-based complex is found to be 270 °C which is found to be maximum for this electrolyte film. Thermal stability is found to be 213, 270, 210, 262 and 215 °C for the films D1, D2, D3, D4, and D5, respectively. It was found that the polymer electrolyte based on the plasticizer EC exhibited better thermal stability than the proposed plasticizer-based samples.

Differential Scanning Calorimetry

The DSC curves of the pure PEO, PVdF-HFP and PEO/PVdF-HFP polymer electrolytes with different plasticizers are shown in Fig. 6.

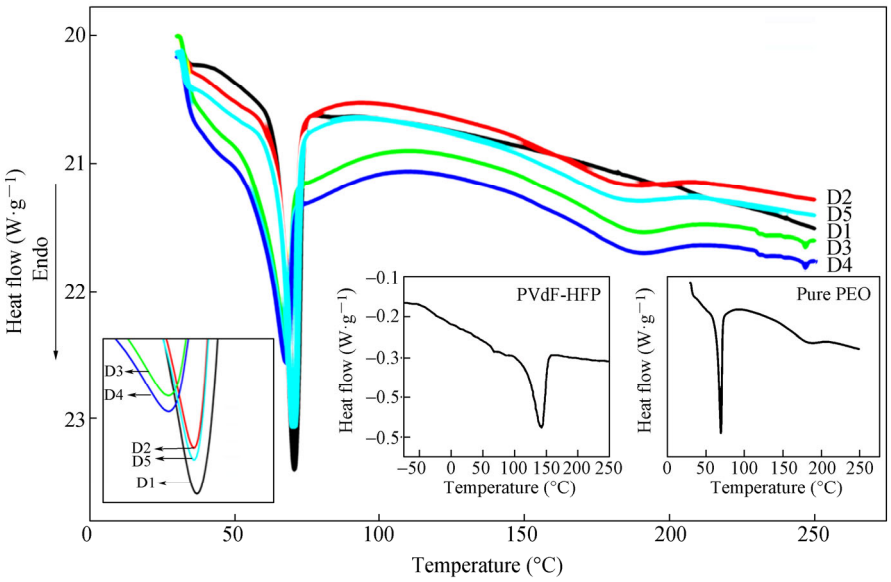

Fig. 6 DSC curves of the pure PEO, PVdF-HFP and prepared polymer electrolytes

The relative percentage of crystallinity has been calculated using Eq. (1):

$$X_c = \frac{\Delta H_m}{\Delta H_m^0} \times 100\% \tag{1}$$

where ΔH_m is the experimental melting enthalpy and ΔH_m^0 is a referenced melting enthalpy. The T_m, T_g and X_c values of the pure PEO are 62.79 °C, −60.03 °C and 56.5%, respectively, and for PVdF-HFP are 112.3 °C, 141.23 °C and 34.3%, respectively. The prepared blends show a phase transition from 53 °C to 78 °C.

The degree of crystallinity of pure PEO and PVdF-HFP is estimated as 56.5% and 34.3%, respectively. It is also estimated for PC, EC, GBL, DEC and DMC based complexes as 34.6%, 32.8%, 39%, 46% and 51%, respectively. The degree of crystallinity of polymer electrolyte decreases with the addition of plasticizer, which causes an increase in the amorphous phase. The polymer chain in the amorphous state is much more flexible than that of the crystalline state. This results in the enhancement of the segmental motion of the polymer. Among the different complexes, the sample prepared with EC shows a minimum T_g value which attributes to its maximum ionic conductivity. The decrease in the T_g value also indicates the decrease of crystallinity upon the addition of plasticizer. This suggests that plasticizer contribute to the reduction of crystal phase.

AFM Analysis

In the present study, two and three dimensional topographic images of the sample D2 having a maximum ionic conductivity are shown in Figs. 7(a) and 7(b).

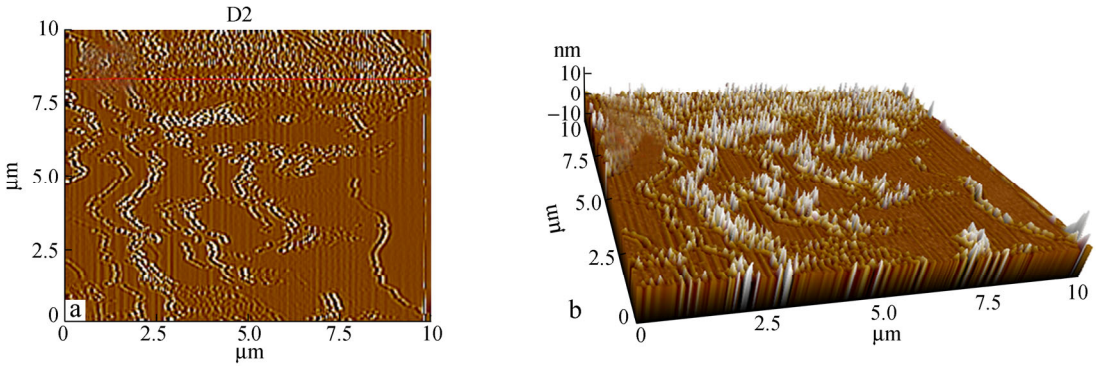

Fig. 7 Topography images of the maximum ionic conductivity sample: (a) 2D image and (b) 3D image

The topographic images clearly show the presence of pores which are responsible for maximum ionic conductivity. The pores are helped to trap the large volume of the liquid in the pores, accounting for the increased conductivity, and the presence of pores in the microstructure is mainly due to solvent removal and by solvent retention ability of the electrolyte system. The average roughness (R_{rms}) was calculated using the Eq. (2):

$$R_{rms} = \left(\frac{1}{N}\right)\sum_{i=1}^{N}|Z_m - Z_i| \tag{2}$$

where N is the number of deviations in height, Z_i from the profile mean value Z_m[48].

The composite polymer electrolyte shows a clear mountain-valley pattern with more number of mountains and valleys. A well defined mountain valley pattern with a roughness RMS value of 1.513 nm is observed for the surface of PEO/PVdF-HFP/$LiClO_4$/EC system. The roughness factor has an important role in the ionic conduction. The roughness value for the polymer electrolyte suggests that there is a good complexation between polymer and the plasticizer used. It is observed that the root mean square roughness of the sample within the scanned area is found to be 2.024 nm. The good miscibility of the plasticizer, lithium salt and the host polymer is very important prerequisite for good ionic conductivity. The roughness value is observed for EC added system that led to the structural modification of the polymer system.

Scanning Electron Microscopy

Scanning electron micrographs of samples PC, EC, GBL, DEC and DMC based samples are shown in Figs. 8(D1)–8(D5), respectively. The chemical bonds and linkages in the polymer complex are affected by the addition of a plasticizer, and two factors that play an important part in enhancing ionic conductivity are the dissociation constant and the dielectric constant of the plasticizer[49]. From Fig. 8, it is observed that electrolyte film is a two-phase system having the polymer and the liquid electrolyte phases. Microstructure shows that the

film is interspersed with pores filled with liquid electrolyte, which form a connected path through the polymer matrix[50]. All the developed electrolytes are found to be homogeneous in appearance. This implies that the polymer and solvent are completely dissolved.

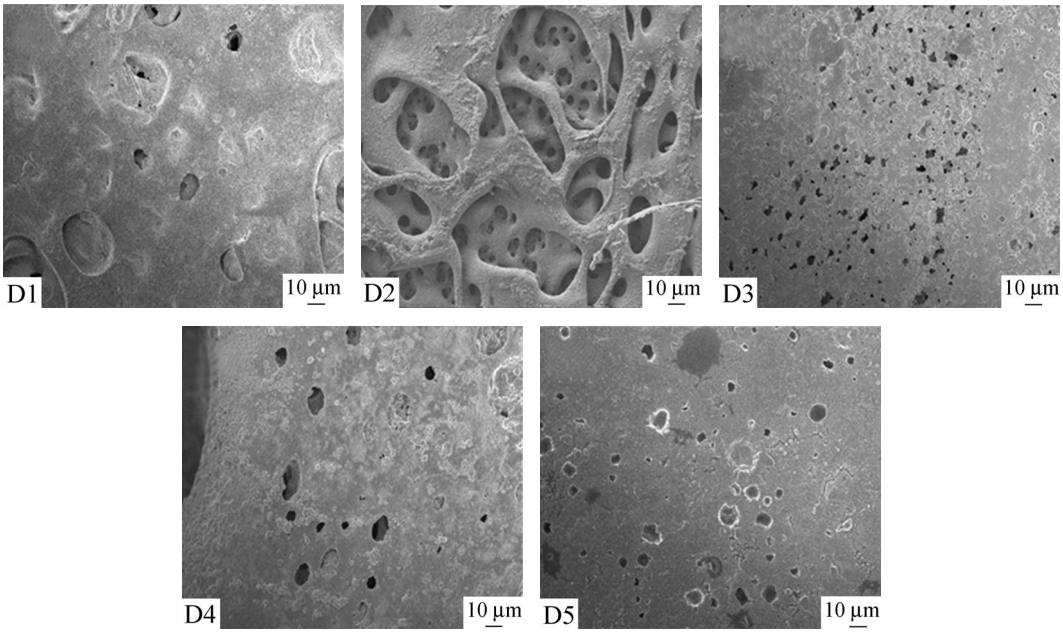

Fig. 8 Scanning electron microscope images of plasticized polymer electrolyte films containing (D1) PC, (D2) EC, (D3) GBL, (D4) DEC and (D5) DMC

Presence of liquid and the solid polymer phases of the electrolyte medium was confirmed from the surface images. Among all the films, D2 has a large number of pores. The increased porosity leads to the entrapment of large volume of the liquid in the cavities accounting for the increased ionic conductivity. The presence of pores in the microstructure is mainly due to the solvent removal[51], increased amorphicity, and solvent retention ability in the electrolyte system. The pores in the micrographs indicate the occurrence of phase separation in the polymer electrolytes. The difference in the pore size is related to the difference in the driving for the phase separation[52]. These results reveal that the morphology of the plasticized films is important and will affect the conductivity of plasticized polymer electrolyte films.

Porosity Measurements

The membrane porosity ε (%) is defined as the volume of pores divided by the total volume of the porous membrane. The weight of liquid contained in the membrane pores can usually be determined by gravimetric method. The porosity percentage of the PEO/PVdF-HFP plasticized membrane was determined using acetone uptake. For this purpose plasticized membrane was soaked in acetone for 1–3 h. The mass of PVdF-HFP plasticized membrane before and after immersion was measured. The porosity (%) of the membrane was calculated using the Eq. (3):

$$\varepsilon\ (\%) = \frac{(W_1 - W_2)/d_w}{(W_1 - W_2)/d_b + W_2/d_p} \times 100 \tag{3}$$

where W_1 is the weight of the wet membrane (mg), W_2 is the weight of the dry membrane (mg), after and before soaking in acetone, whereas d_b and d_p are density of the acetone and polymer respectively.

Evaluation in Li/LiFePO$_4$ Cell

Galvanostatic charge-discharge (GCD) characteristics of the plasticized polymer electrolyte membrane were evaluated in a half cell configuration in which $LiFePO_4$ and lithium foil was used as cathode and anode, respectively. Figure 9 shows the capacity versus voltage profile of the cell at 0.1 C rate with the operating potential range from 2.5 V to 4.5 V.

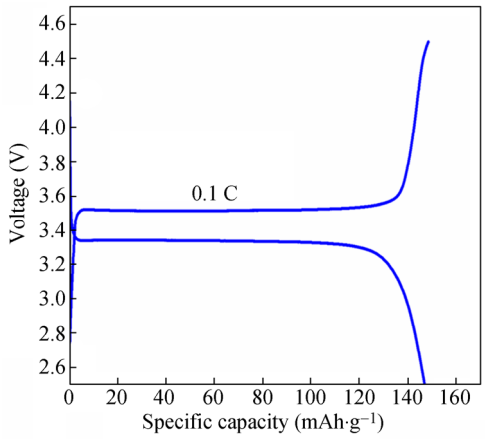

Fig. 9 Charge discharge properties of $LiFePO_4$/PPEs/Li cells with polymer electrolytes based on PEO/PVdF-HFP blended with EC at room temperature

It was noted that the cell with the PEO/PVdF-HFP/EC plasticized membrane, delivered a discharge capacity of 148 mAh·g^{-1} at 0.1 C. This value mainly depends on the electrode material used for the cell fabrication; in the present investigation the electrode used has a theoretical capacity of 170 mAh·g^{-1}. The obtained value in the present study is close to the above said theoretical value of the $LiFePO_4$ electrode.

The cell retained its performance even after many cycles tested at different current rates. The cell performance obtained at different current rates is shown in Fig. 10 and the results confirmed good cycle life capability of the cell and a relatively high specific capacity, 148 and 137 mAh·g^{-1}, under low and medium C rates (0.1 C–0.3 C), respectively. It was observed that the significant capacity decreased to 92 mAh·g^{-1} at the 0.5 C rate and also to 66 mAh·g^{-1} at the 1 C rate. However, the return to the lower current density (0.1 C) results in an increase in specific capacity (141 mAh·g^{-1}).

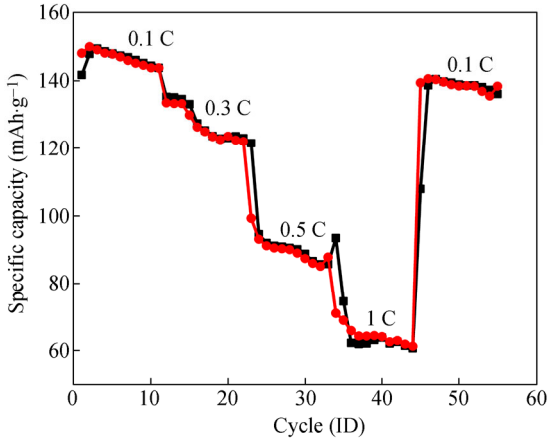

Fig. 10 Relationship between cycle performance and C rates of cells assembled with separators

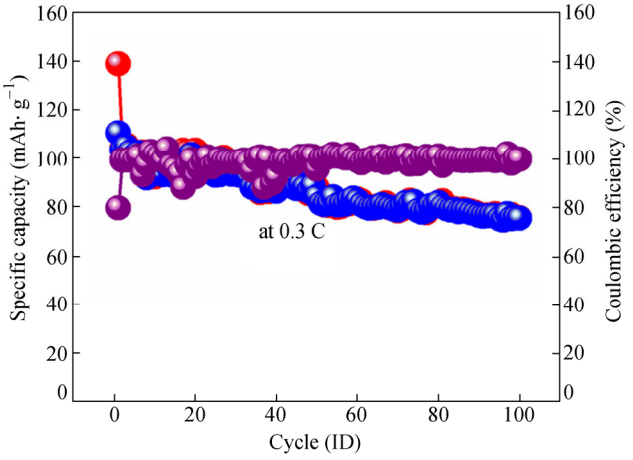

Fig. 11 Cycle performance of cells with coulombic efficiency at 0.3 C rate, assembled with separators at 30 °C

Thus, the voltage plateaus during charge-discharge process remain stable throughout cycling; the good performance of the PPEs can be attributed to the high ionic conductivity of the membrane. The above results demonstrated the good electrochemical stability of the PEO/PVdF-HFP plasticized polymer electrolyte; this is another important factor that contributes to the cycle life.

Cycle life of the cell was evaluated at 0.3 C rates (Fig. 11). The cell showed a charge and discharge capacity of 116 and 104 $mAh \cdot g^{-1}$, respectively, resulting in a coulombic efficiency of 92%. In subsequent cycles, the coulombic efficiency increased to 98.7% at the 100^{th} cycle. The reversible capacity is not low, which is a good result and provides promising prospects.

CONCLUSIONS

Polymer electrolytes comprising EC, PC, GBL, DMC and DEC complexed with PEO (6.25)/PVdF-HFP (18.75)/$LiClO_4$ (8) system were prepared using solvent casting technique. Complexation of the polymer matrices was ascertained by XRD and FTIR analyses. Ionic conductivity of the polymer electrolytes was measured in the range of 303–343 K. The maximum conductivity value was obtained for EC-based complex because of the higher dielectric constant as compared to other plasticizers used in the present study. The temperature-dependent ionic conductivity plots of the electrolyte films exhibited the Arrhenius relation. The ionic transport of the electrolytes was discussed on the basis of free volume model. Thermal stability of the prepared complexes was observed from TG-DTA thermograms. Thermal stability of the sample having PEO (6.25)/PVdF-HFP (18.75)/$LiClO_4$ (8)/EC (67) was found to be at 270 °C. Two and three dimensional topographic images of the sample with incorporation of EC were studied by AFM to observe the roughness parameter of the blended electrolytes. Electron micrographs showed uniform distribution of one polymer in the other which confirms the compatibility of the blend components. Attainment of smooth surface morphology on the addition of plasticizer EC also suggested the enhancement of degree of amorphicity. The polymer gel electrolyte incorporated with plasticizer EC in PEO/PVdF-HFP based membranes produced stable charge discharge characteristics when evaluated as separator-cum-electrolyte in a lithium ion cell. It is concluded that the PEO/PVdF-HFP/$LiClO_4$/EC based plasticized can be used as a promising candidate for rechargeable lithium-ion batteries.

REFERENCES

1 van Vliet, O., Brouwer, A.S., Kuramochi, T., van den Broek, M. and Faaij, A., J. Power Sources, 2011, 196: 2298
2 Goodenough, J.B. and Kim, Y., Chem. Mater., 2010, 22: 587
3 Goriparti, S., Miele, E., de Angelis, F., di Fabrizio, E., Zaccaria, R.P. and Capiglia, C., J. Power Sources, 2014, 257: 421
4 Vincent, C.A. and Scrosati, B., "Modern batteries: An introduction to electrochemical power sources", Butterworth-Heinemann, London, 1997
5 Armand, M. and Tarascon, J.M., Nature, 2008, 451: 652
6 Kalhammer, F.R., Solid State Ionics, 2000, 135: 315
7 Kunze, M., Karatas, Y., Wiemhofe, H.D., Ecker, H. and Schonh, M., Phys. Chem. Chem. Phys., 2010, 12: 6844
8 Saikia, D., Chen, Y.H., Pan, Y.C., Fang, J., Tsai, L.D., Fey, G.T.K. and Kao, H.M., J. Mater. Chem., 2011, 21: 10542
9 Costa, C.M, Rodrigues, L.C., Sencadas, V., Silva, M.M. and Lanceros-Méndez S., Solid State Ionics, 2012, 217: 19
10 Ha, H.J., Kwon, Y.H., Kim, J.Y. and Lee, S.Y., Electrochim. Acta, 2011, 57: 40
11 Chen, Y.T., Chuang, Y.C., Su, J.H., Yu, H.C. and Chen-Yang, Y.W., J. Power Sources, 2011, 196: 2802
12 Zhang, J., Huang, X., Wei, H., Fu, J., Huang, Y. and Tang, X., J. Appl. Electrochem., 2010, 40: 1475
13 Patel, M., Patel, M.U.M. and Bhattacharyya, A.J., Chem. Sus. Chem., 2010, 3: 1371
14 Sarnowska, A., Polska, I., Niedzicki, L., Marcine, M. and Zalewska, A., Electrochim. Acta, 2011, 57: 180
15 Rajendran, S., Prabhu, M.R. and Rani, M.U., J. Power Sources, 2008, 180: 880

16 Saikia, D., Wu, H.Y., Pan, Y.C., Lin, C.P., Huang, K.P., Chen, K.N., Fey, G.T.K. and Kao, H.M., J. Power Sources, 2011, 196: 2826
17 Rajendran, S. and Bama, V.S., J. Non-Cryst. Solids, 2010, 356: 2764
18 Sun, X.G., Liu, G., Xie, J.B. and Han, Y.B., Solid State Ionics, 2004, 175: 713
19 Kim, K.M., Park, N.G., Ryu, K.S. and Chang, S.H., Electrochim. Acta, 2006, 51: 5636
20 Singh, T.J. and Bhat, S.V., J. Power Sources, 2004, 129: 281
21 Vignarooban, K., Dissanayake, M.A.K.L., Albinsson, I. and Mellander, B.E., Solid State Ionics, 2014, 266: 25
22 Pitawala, H.M.J.C., Dissanayake, M.A.K.L., Seneviratne, V.A., Mellander, B.E. and Albinson, I., J. Solid State Electron., 2008, 12: 783
23 Shin, J.H., Jung, S.S., Kim, K.M. and Ahn, J.H., J. Mater. Sci.: Mater. Electron., 2002, 13: 727
24 Fan, L.Z., Dang, Z.M., Nan, C.W. and Li, M., Electrochim. Acta, 2002, 487: 205
25 Pradeepa, P., Edwinraj, S., Sowmya, G., Kalaiselvimary, J. and Prabhu, M.R., Mater. Sci. Eng., B., 2016, 205: 6
26 Pradhan, D.K. and Tripathy, S.N., Adv. Chem. Sci., 2013, 2: 2013
27 Prajapati, G.K., Rosh, R. and Gupt, P.N., J. Phys. Chem. Solids, 2010, 71: 1717
28 Noor, S.A.M., Ahmad, A., Talib, I.A. and Rahman, M.Y.A., Ionics, 2010, 16: 161
29 Simon, G.P., Shen, Z. and Cheng, Y.B., Eur. Polym. J., 2003, 39: 1924
30 Kumar, K.K., Ravi, M., Pavani, Y., Bhavani, S., Sharma, A.K. and Narasimha Rao, V.V.R., Physica B, 2011, 406: 1706
31 Naveen Kumar, K., Sivaiah, K. and Buddhudu, S., J. Lumin., 2014, 147: 316
32 Ulaganatha, M. and Rajendran, S., Ionics, 2010, 16: 515
33 Shukla, N. and Thakur, A.K., Solid State Ionics, 2010, 181: 921
34 Rajendran, S. and Sivakumar, P., Physica B, 2008, 403: 509
35 Rajendran, S. and Prabhu, M.R., J. Appl. Electrochem., 2010, 40: 327
36 Lee, T.K., Afiqah, S., Ahmad, A., Dahlan, H.M. and Rahman, M.Y.A., J. Solid State Electrochem., 2012, 16: 2251
37 Coates, J., "Interpretation of IR spectra, a particular approach", Wiley, Chichester, 2000
38 Khanmirzaei, M.H. and Ramesh, S., Int. J. Electrochem. Sci., 2013, 8: 9977
39 Subbu, C., Rajendran, S., Kesavan, K. and Premila, R., Ionics, 2016, 22: 229
40 Raghavan, P., Manue, J., Zhao, X., Kim, D.S., Ahn, J.H. and Nah, C., J. Power Sources, 2011, 196: 6742
41 Chandra Sekhar, P., Naveen Kumar, P. and Sharma, A.K., IOSR J. Appl. Phys., 2012, 2: 1
42 Rajendran, S., Sivakumar, M. and Subadevi, R., Mater. Lett., 2004, 58: 641
43 Saikia, D., Ho, S.Y., Chang, Y.J., Fang, J., Tsai, L.D. and Kao, H.M., J. Membr. Sci., 2016, 503: 59
44 Sun, H., Lu, B.Y., Hu, D.F., Duan, X.M., Xu, J.K., Zhen, S.J., Zhang, K.X., Zhu, X.F., Dong, L.Q. and Mo, D.Z., Chinese J. Polym. Sci., 2015, 33: 1527
45 Saito, Y., Kataoka, H., Quartarone, E. and Mustarelli, P., J. Phys. Chem. B., 2002, 106: 7200
46 Ramesh, S. and Arof, A.K., J. Power Sources, 2001, 99: 41
47 Jayanth, S., Arulsankar, A. and Sundaresan, B., Appl. Phys. A., 2016, 122: 109
48 Stephen, A.M., Saito, Y., Muniyandi, N., Ranganathan, N.G., Kalyanasundram, S. and Elizabeth, R., Solid State Ionics, 2002, 148: 467
49 Kumar, M. and Sekhon, S.S., Ionics, 2002, 8: 223
50 Kim, C.S. and Oh, S.M., Electrochim. Acta, 2000, 45: 2101
51 Ulaganathan, M., Nithya, R., Rajendran, S. and Raghu, S., Solid State Ionics, 2012, 218: 7
52 Rajendran, S., Prabhu, M.R. and Rani, M.U., Int. J. Electrochem. Sci., 2008, 3: 282